Automatic segmentation of tooth images: Optimization of multi-parameter image processing workflow

Giovani Bressan Fogalli[1,2] , Sérgio Roberto Peres Line[1] and Daniel Baum[2]

[1]Department of Biosciences, Piracicaba Dental School, State University of Campinas, Brazil
[2]Department of Visual and Data-Centric Computing, Zuse Institute Berlin, Germany

Abstract

The development of specific algorithms in image processing are usually related to dataset characteristics. Those characteristics will influence the number of instructions required to solve a problem. Normally, the more complex a set of instructions is, the more parameters need to be set. Dealing with such degrees of freedom, sometimes leading to subjective decision making, is time-consuming and frequently leads to errors or sub-optimal results of the developed model. Here, we deal with a model for segmentation of masks of tooth images containing a pattern of bands called Hunter-Schreger Bands (HSB). They appear on tooth surface when lit from the side. This segmentation process is only one step of a pipeline whose overall goal is human biometric identification to be used, e.g., in forensics. The segmentation algorithm, which exploits the anisotropy of the image, uses several parameters and choosing the optimal combination of them is challenging. The aim of this work was to utilize visual data analysis tools to optimize the chosen parameters and to understand their influence on the performance of the algorithm. Our results reveal that a slightly better combination of parameter values can be found starting from the experimentally determined initial parameters. This approach can be repeatedly performed to achieve even better parameterizations. To more deeply understand the influence of the parameters on the final result, more sophisticated visual interaction tools will be explored in future work.

1. Introduction

Tooth enamel is the hardest tissue in human body and can bear high temperatures, wearing, humidity, pressure [SS95, VdlHM*00], and hold their characteristics for thousand of years, as supported by teeth found in fossils [vK94]. There is an optical phenomenon at tooth enamel surface level called Hunter-Schreger Bands (HSB), which occurs when a strong light is set on the side of a tooth. This phenomenon is present in mammals and has been shown to resemble the fingerprint pattern, although it has a predominant horizontal orientation [vKHR11, vKRP87]. Previous work also showed the potential of HSB to be harnessed as a new method for human identification, since HSB pattern seems to be unique for each tooth [RL06]. A specific pipeline is currently in development for biometric application of this idea. The main workflow begins with a photograph of the tooth crown illuminated laterally, enhancement of HSB [AFL18], segmentation of HSB region, filtration, feature extraction, and matching. The main problem for the segmentation step is the subjective human perception of the useful HSB region borders, which leads eventually to either quality degradation (for too large selected regions) or loss of information (for too small selected regions), and also is a time-consuming task. To automate the process, a specific image processing pipeline was developed, which we call anisotropy-based segmentation. It involves three parameters, the tuning of which to achieve the best possible model performance is the goal of the presented work.

2. Methods

To tackle the segmentation problem, we used ground truth segmentation masks that were created using manual segmentation and iterative filtering. As result of the iterative filtering, we gradually reduce the mask region size up to the point where the filtered HSB were suitable for biometric analysis. Our dataset so far consists of 124 images (4 different images for each of 31 extracted teeth). Our anisotropy-based segmentation resizes the initial image, performs edge-detection, blurring, and subtracts the horizontal from the vertical orientation component. The resulting heatmap highlights dense horizontal features in the tooth image, in particular the HSB. The heatmap is then passed through normalization procedures, has its background removed in two steps and its shape smoothed. In the end, the mask is resized to the original image size for segmenting fore- and background. Examples are shown in Fig. 1. The algorithm has three sensitive parameters: u is linked to the initial image size reduction. The higher u is, the larger is the resized image; $\frac{k_x}{k_y}$ is the blurring operator shape; and α is the factor by which mask shape borders are smoothed. The higher α is, the less the mask shape is smoothed. For evaluation of our automated segmentation results, we used a combination of Intersection over Union (IOU), Exclusive manual segmentation over Union (EMSOU), and Exclusive automated segmentation over Union (EASOU): $IOU + EMSOU + EASOU = 1$, where EMSOU and EASOU are components of the Jaccard dis-
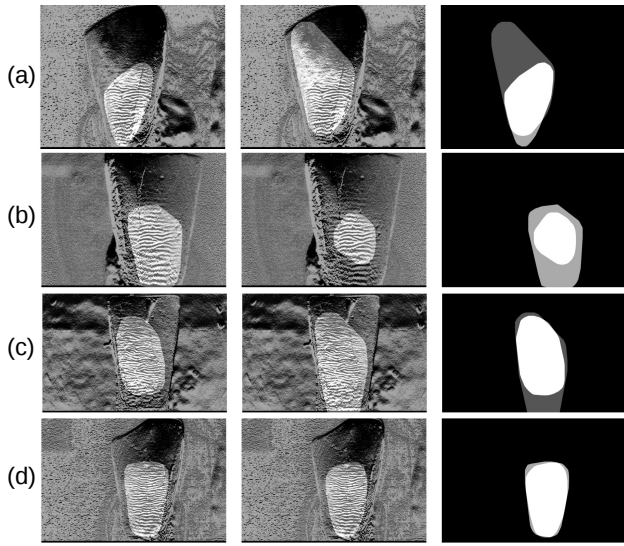
Figure 1: *Examples of HSB segmentation. Left to right: ground truth; automatic segmentation; overlap between masks (light gray - ground truth; dark gray - automatic mask). (a) Too large region. (b) Too small region. (c) Slightly larger region. (d) Desirable result.*

Figure 2: *Scatter plots of all descriptors relations according to parameters $\frac{k_x}{k_y}$ (a,b,c), u (d,e,f), and α (g,h,i). The ⋆ symbol represents the best model setting.*

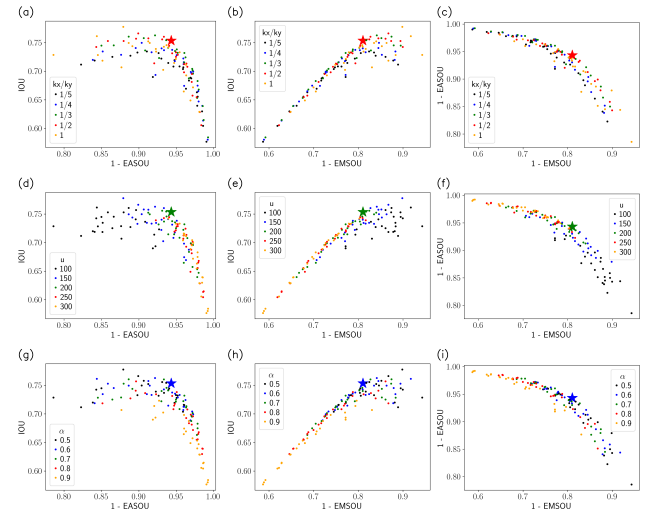**Figure 3:** *Boxplots of parameters $\frac{k_x}{k_y}$ (a), u (b), and α (c).*

tance [LW71]. From manual adjustment of the parameters by experimentation, reference values for each parameter were obtained. We tested variations of each parameter in the close neighborhood to observe the impact on the model. From this manual testing, suitable parameter values were selected: $\frac{k_x}{k_y} = \frac{1}{3}$; $u = 200$; $\alpha = 0.7$. Around these initial values, further candidate values were sampled. Values for the dependent variables k_x and k_y were chosen as $(k_x, k_y) \in \{(86, 86), (61, 122), (50, 150), (43, 172), (39, 195)\}$, resulting in $\frac{k_x}{k_y} \in \{1, \frac{1}{2}, \frac{1}{3}, \frac{1}{4}, \frac{1}{5}\}$. For the independent variables u and α, we chose the following values: $u \in \{100, 150, 200, 250, 300\}$, $\alpha \in \{0.5, 0.6, 0.7, 0.8, 0.9\}$. As result, we obtained 125 parameter combinations, all of which were tested on the whole dataset.
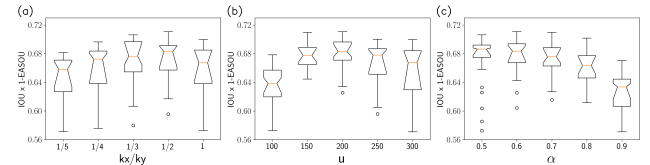
3. Results

The best model can be achieved by maximizing IOU and minimizing EMSOU and EASOU. Because EASOU is more critical to model degradation, and for dimensionality reduction purpose, we opted to assess model performance by maximizing the function $IOU \times (1 - EASOU)$.

The scatter plots (Fig. 2) show a negative correlation between IOU and EASOU, and EMSOU and EASOU, while IOU and EMSOU have a positive correlation. From these correlations, we can interpret that while increasing automated masks size returns a higher IOU and reduces the difference between manual and automated masks for some samples, it also increases the chances of selecting too large masks on other samples.

Regarding testing of the parameters, we found a slightly better combination of parameters than the one we started from: $\frac{k_x}{k_y} = \frac{1}{2}$, $u = 200$, and $\alpha = 0.6$. The u parameter showed a clear trend with overlapping clusters through the tested values, where a smaller u

seems to increase IOU, but also increases EASOU. The α presented a weak trend over the tested values, where clusters mostly overlapped each other, where lower values affected IOU positively. Finally, $\frac{k_x}{k_y}$ ratio appeared to have no clustering, but values between $\frac{1}{2}$ and $\frac{1}{3}$ seemed to achieve the best results. This information can be confirmed by the boxplots (Fig. 3), which depict the distribution of results for varying the three parameters, and give hints to better approximations if the processing of searching parameter values around the optimized ones is repeated within smaller ranges.

4. Limitations and future works

Even with improved results, there are still segmented images with poor quality (Fig. 1a,b). Of course, there are methods to work around these problems that could be added to the main biometric pipeline, e.g. post-segmentation quality control. However, those methods depend on repetition of steps, thus increasing the computational cost. Therefore, in future works, we would like to make use of visual data analysis frameworks like link-and-brush to further explore the relation between computational parameters and the resulting segmentations. In particular, it might be interesting to look at derived attributes of the segmented masks including shape descriptors, curvature, and orientation together with a direct visualization of the segmented shape. To this end, parallel coordinate plots might be well suited to depict both the parameter space and the attribute space, and allow one to explore their mutual influence. This might lead to a further optimization of the parameters regarding the performance of the overall biometric identification pipeline.

Acknowledgements

References

[AFL18] ARRIETA Z. L., FOGALLI G. B., LINE S. R. P.: Digital enhancement of dental enamel microstructure images from intact teeth. *Microscopy Research and Technique 81*, 9 (2018), 1036–1041. URL: https://analyticalsciencejournals.onlinelibrary.wiley.com/doi/abs/10.1002/jemt.23070, doi:https://doi.org/10.1002/jemt.23070. 1

[LW71] LEVANDOWSKY M., WINTER D.: Distance between sets. *Nature 234*, 5323 (Nov. 1971), 34–35. URL: https://doi.org/10.1038/234034a0, doi:10.1038/234034a0. 2

[RL06] RAMENZONI L. L., LINE S. R.: Automated biometrics-based personal identification of the Hunter-Schreger bands of dental enamel. *Proceedings of the Royal Society B: Biological Sciences 273*, 1590 (Jan. 2006), 1155–1158. URL: https://doi.org/10.1098/rspb.2005.3409, doi:10.1098/rspb.2005.3409. 1

[SS95] SWEET D., SWEET C.: DNA analysis of dental pulp to link incinerated remains of homicide victim to crime scene. *Journal of forensic sciences 40 2* (1995), 310–4. 1

[VdlHM*00] VALENZUELA A., DE LAS HERAS S. M., MARQUES T., EXPOSITO N., BOHOYO J. M.: The application of dental methods of identification to human burn victims in a mass disaster. *International Journal of Legal Medicine 113*, 4 (June 2000), 236–239. URL: https://doi.org/10.1007/s004149900099, doi:10.1007/s004149900099. 1

[vK94] V. KOENIGSWALD W.: U-shaped orientation of Hunter-Schreger bands in the enamel of moropus (mammalia: Chalicotheriidae) in comparison to some other Perissodactyla. *Annals of Carnegie Museum 63* (1994), 49–65. 1

[vKHR11] V. KOENIGSWALD W., HOLBROOK L. T., ROSE K. D.: Diversity and evolution of hunter-schreger band configuration in tooth enamel of perissodactyl mammals. *Acta Palaeontologica Polonica 56*, 1 (2011), 11–32. 1

[vKRP87] V. KOENIGSWALD W., RENSBERGER J. M., PRETZSCHNER H. U.: Changes in the tooth enamel of early Paleocene mammals allowing increased diet diversity. *Nature 328*, 6126 (July 1987), 150–152. URL: https://doi.org/10.1038/328150a0, doi:10.1038/328150a0. 1